Phys. Med. Biol., 1992, Vol. 37, No 10, 1873–1882. Printed in the UK

Photon absorption measurements of bone density in the presence of scattered radiation

M J Mooney and R D Speller

Medical Physics Department, University College and Middlesex School of Medicine, 11–20 Capper Street, London WC1E 6JA, UK

Received 12 March 1992, in final form 11 June 1992

Abstract. Bone density measurements are frequently carried out using photon absorptiometry techniques. The analysis of data collected in this way depends upon scatter-free detector signals. In practice the detector and source collimation lead to high levels of scattered radiation being detected. An analysis of the problem using photon transport computer models has shown that the current systems are reasonably insensitive to the scatter contribution except where patient changes occur over a long series of measurements or where new results taken with DEXA are compared with those taken on older systems such as DPA. This is frequently the case since the major body of data related to serial bone density measurements has been achieved with DPA. Inclusion of scattered radiation in the bone density calculations can lead to a 0.5–3.5% reduction between system types. Patient size changes could lead to a reduction in bone density of 0.5% (femoral neck measurement) to 1% (lumbar spine measurement).

1. Introduction

Evaluation of osteoporotic patients has been made by a variety of methods over the last three decades (Speller *et al* 1989). However, the two major methods are those of quantitative computed tomography (QCT) and photon absorptiometry (PA). Recently there has been a significant improvement in the precision available from PA systems with the introduction of Dual Energy x-ray Absorption (DEXA) (Cullum *et al* 1989). Absorptiometers use collimated sources and detectors to scan various absorption paths through the patient; paths containing bone can be analysed to reveal the bone mass per unit area (see for example Cameron and Sorenson 1963, Roos and Sköldborn 1974). Using two radiation energies allows the system to take account of different thickness patient sections and has therefore led to systems that are more convenient to use and which can examine some of the more clinically relevant bone sites. Accuracy and precision are important in bone densitometry; accuracy for comparative measurements with other systems, and precision for serial measurements. Measurement of bone density is important since 30–35% of the bone strength is attributable to density as measured by PA (Haddaway *et al* 1989). The analysis for dual energy absorptiometry is very similar to the early work of Roos and Sköldborn (1974), and is based upon the principle of narrow beam exponential attenuation. An important point is that the theory assumes the only detected photons are primary photons which have not undergone any scattering process. In clinical bone densitometers this is not the case. Instead, collimation is such that a considerable

0031-9155/92/101873+10$04.50

scattered radiation flux contributes to the signals that are finally analysed to calculate bone mass.

This paper analyses the magnitude of this effect and the changes in bone density or mass that would be attributed to the patient due to the effect of including scattered radiation. The approach that has been used is to follow photon histories using a Monte Carlo computer code. The advantage of this technique is that individual photons can be classified according to their history and therefore the number of primary photons and the number of scattered photons can be recorded separately. The particular code employed has been modified from routines used to study Compton scatter densitometry (Speller and Horrocks 1988, Koligliatis 1990).

2. The photon transport model

Photon histories are followed by making decisions about the location and type of interactions by the random sampling of probability distributions (Raeside 1976). In the model Rayleigh scattering, Compton scattering and photoelectric absorption are the only interactions that have been used. Two rejection techniques (Cashwell and Everett 1959, Williamson and Morin 1983) have been used to sample scattering events and the result of a photoelectric interaction is assumed to be total absorption.

2.1. Phantoms

Photons have been traced through semi-infinite elliptical phantoms that represent measurement sites containing the neck of the femur and the lumbar spine. All phantoms were composed of four materials; cortical bone, trabecular bone, muscle tissue and adipose fat. The elemental compositions have been taken from ICRP reference man (ICRP 1975) and the appropriate attenuation data have been taken from Storm and Israel (1970) and Hubbell (1969). The general geometries and dimensions described in the computer models are given in figure 1 and table 1, respectively. All phantoms contain unit density trabecular bone.

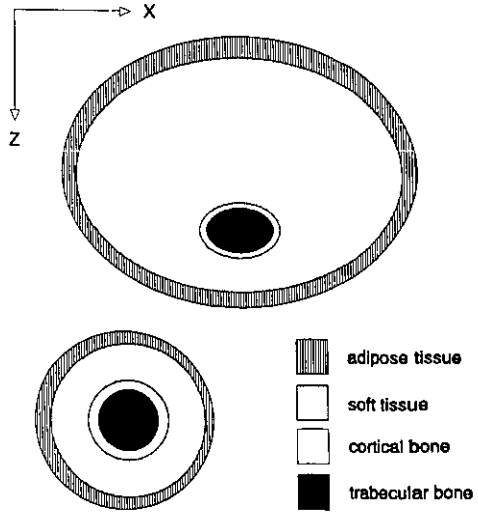

Figure 1. Phantoms used in the computer simulations representing the femoral neck and lumbar spine sites. Each phantom consists of four tissue types and the asymmetry is intended to represent the normal arrangement of these tissues.

Table 1. x- and z-semi-axes dimensions of the tissue components in the femoral neck and lumbar spine phantoms used in the computer simulations.

Femoral neck site measurement phantoms

Phantom	Adipose tissue		Soft tissue		Cortical bone		Trabecular bone	
	x (cm)	z (cm)	x (cm)	z (cm)	x (cm)	z (cm)	x (cm)	z (cm)
1	5.25	5.25	3.98	3.98	3.25	3.25	2.75	2.75
2	6.25	6.25	4.73	4.73	3.25	3.25	2.75	2.75
3	7.25	7.25	5.49	5.49	3.25	3.25	2.75	2.75
4	8.25	8.25	6.25	6.25	3.25	3.25	2.75	2.75
5	9.25	9.25	7.01	7.01	3.25	3.25	2.75	2.75

Lumbar spine site measurement phantoms

Phantom	Adipose tissue		Soft tissue		Cortical bone		Trabecular bone	
	x (cm)	z (cm)	x (cm)	z (cm)	x (cm)	z (cm)	x (cm)	z (cm)
1	13.00	9.79	11.96	8.67	3.20	2.10	3.00	1.90
2	14.00	10.55	12.88	9.33	3.20	2.10	3.00	1.90
3	15.00	11.30	13.80	10.00	3.20	2.10	3.00	1.90
4	16.00	12.05	14.72	10.67	3.20	2.10	3.00	1.90
5	17.00	12.80	15.64	11.33	3.20	3.10	3.00	1.90

2.2. Systems

Two absorption systems have been modelled. The isotope dual energy absorptiometer (DPA) has been included as this is the type of system that has created the current data base on normal and pathological bone density and therefore warrants investigation. The DEXA system is now considered the replacement system for bone density measurements. Figures 2 and 3 show the geometries used in the computer simulations. The dimensions are based on the Norland 2600 DPA (^{153}Gd isotope source) and the Norland XR26 DEXA, but are representative of most current DPA and DEXA systems. The x-ray spectrum for the DEXA system was modelled as 100 kV_p filtered with 0.6 g cm^{-2} of samarium calculated from Birch and Marshall (1979). Electronic windows of 20% were used for the DPA ^{153}Gd low and high energy spectrum components. Photon deposition in the DEXA detector components were also modelled. All computer runs considered at least 2×10^6 photons incident on the phantom at each point in the scanned profile. The scan width encompassed a large soft tissue background either side of the bone and each scan point was separated by 0.4 cm. All jobs were run on SUN Sparcstations within the department.

3. Analysis and results

Typical detected count scans from the computer model are shown in figures 4(*a*) and (*b*). It can be seen that there is a general increase in absorption as the tissue thickness increases and a sudden marked increase in absorption at the bone edges, which contain cortical bone only. There is a marked increase in scatter at the bone edges, with respect to the primary transmission, and also within the bone width. This may be due to two causes: firstly the increased density at these points increases

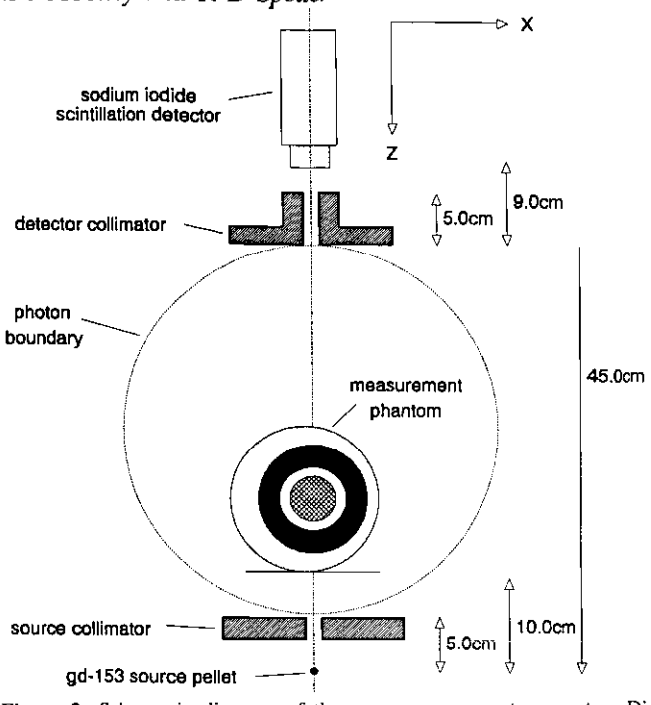

Figure 2. Schematic diagram of the DPA measurement geometry. Dimensions represent the Norland 2600. Source collimator diameter = 0.3 cm, detector collimator diameter = 0.8 cm.

the probability of a Compton interaction, and secondly the increase in absorption at these points increases the proportion of scatter. The scatter profile, particularly at low energy, demonstrates a very similar shape to the transmission beam profile. This indicates that multiple scattering must be a small component and since the width of the profile is altered very little, it must also be primarily low-angle forward scatter. The asymmetrical shape of the graphs for the femoral neck site is attributable to the offset position of the bone within the phantom. Both the total detected counts and the scattered counts have been generated for the DPA and DEXA systems for both the femoral neck and lumbar spine sites. In general all results have a similar behaviour although the proportion of scatter to transmission does vary between phantoms and systems. The proportion of scatter for the DPA system ranges from 7 to 25%, and for the DEXA system ranges from 6 to 20%.

The effects of scatter on bone density measurements are best evaluated by considering the equation used in the analysis; in the case of narrow beam geometry where scatter is not included, it can be shown that (Roos and Sköldborn 1974)

$$m_b = \frac{N - D_{sf} m_f}{D_{sb}} \tag{1}$$

where

$$\begin{aligned} D_{sb} &= \mu_s^h \mu_b^l - \mu_s^l \mu_b^h \\ D_{sf} &= \mu_s^h \mu_f^l - \mu_s^l \mu_f^h \end{aligned} \tag{2}$$

and

$$N = \mu_s^h \ln\left(\frac{I_0^l}{I^l}\right) - \mu_s^l \ln\left(\frac{I_0^h}{I^h}\right). \tag{3}$$

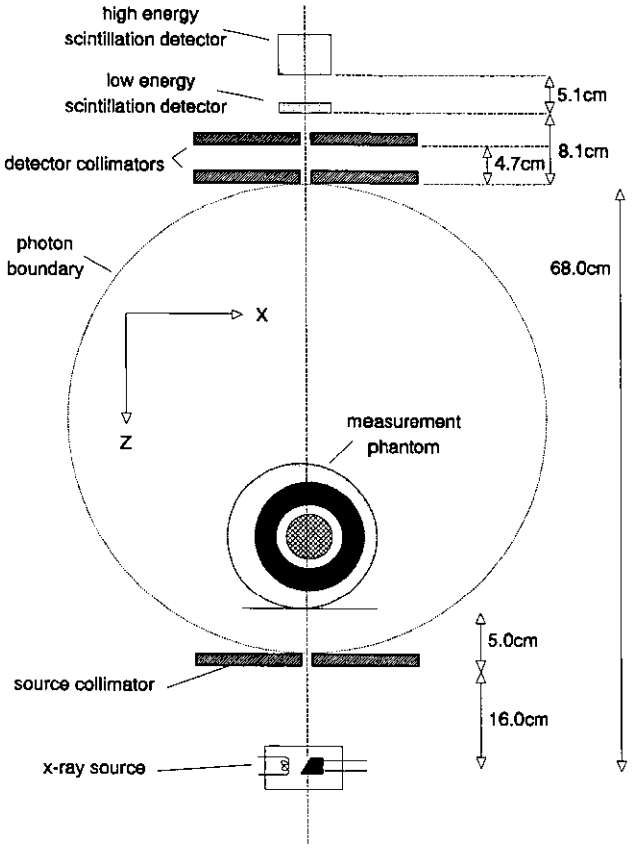

Figure 3. Schematic diagram of the DEXA measurement geometry. Dimensions represent the Norland XR26. Source collimator diameter = 0.4 cm, detector collimator diameter = 0.8 cm.

I and I_0 are transmitted intensity with bone and without bone tissue present in the x-ray beam path, respectively. μ_f, μ_s and μ_b are the mass attenuation coefficients of fat, soft tissue and bone, respectively ($cm^2\ g^{-1}$) and m_f, m_s and m_b are the masses of tissue per unit area in the radiation path ($g\ cm^{-2}$). Symbols with a superscript h are for the high energy beam component and symbols with the superscript l refer to the low energy beam component.

Calculation of m_b requires the profile representing the values of N to be plotted versus measurement point (figure 5) where the presence of bone produces an increase in the value of N. As shown in figure 5, a baseline is drawn beneath these values connecting the values of N produced by soft tissue and fat on either side of the bone. This line accounts for the contribution of any fat tissue assuming the distribution of the fat is even. Integrating the area above the baseline produces a value, A, which is given by

$$A = \int_{p_1}^{p_n} D_{sb} m_b \, dx = D_{sb} \int_{p_1}^{p_n} m_b \, dx = D_{sb} M_b \tag{4}$$

where A is the area under the N versus position curve in $cm^3\ g^{-1}$ and M_b is the mass of bone along the measurement path in $g\ cm^{-1}$.

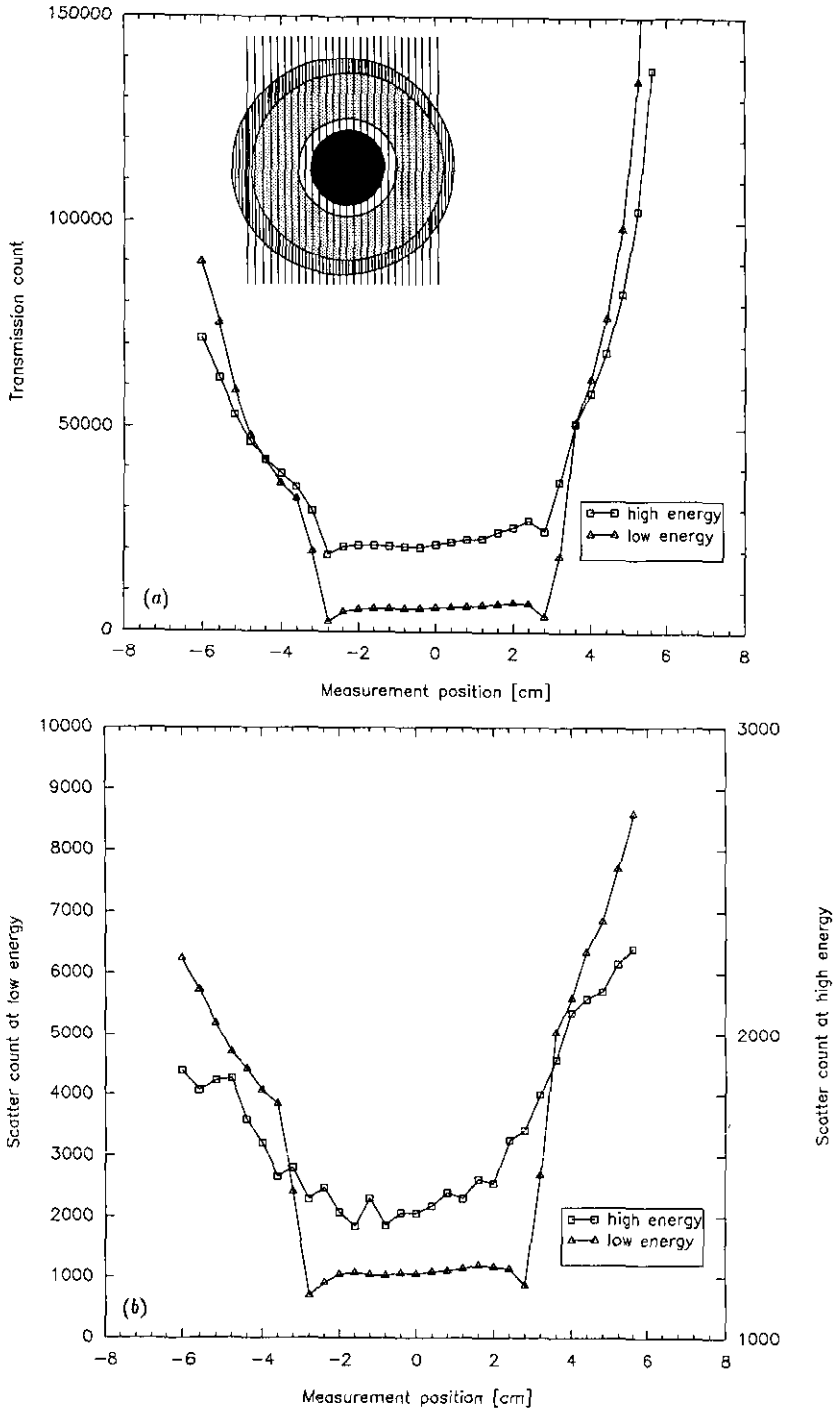

Figure 4. (*a*) Transmitted primary photons for the DPA system from the computer simulation. The phantom studied is a size 3 femoral neck. Both high and low energy beams have been shown. Insert shows the beam paths at each scan interval of 0.4 cm. (*b*) Scattered photons detected for the same phantom and conditions as for (*a*). Left axis shows the low energy scatter count and the right axis shows the high energy scatter count.

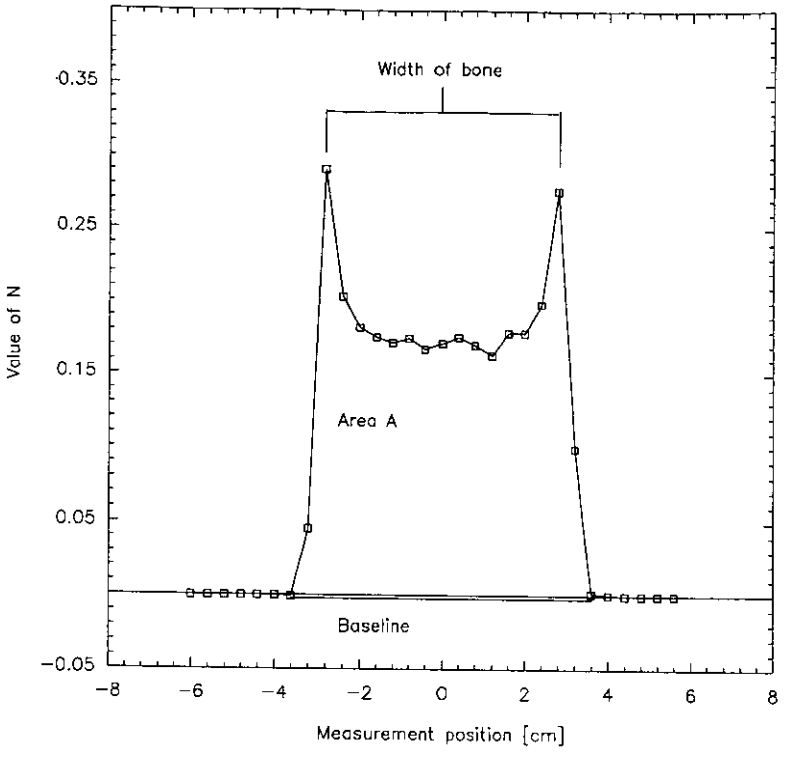

Figure 5. Typical plot of the variable N at different positions in the scan profile. The plot indicates the position of the base line and the area A used to calculate the bone mass per unit area.

This analysis assumes that scattered photons do not contribute to the detected signal. If applied to a signal containing a scattered component it is possible to 'calibrate out' any scattered contribution for a given sized patient. However, if the 'calibration' conditions differ from the clinical measurement conditions, errors will be introduced due to the change in the scatter component. As serial measurements are taken over a long period of time, patient sizes may change and therefore the volume of tissue irradiated will also change. Alternatively, if comparisons are made between different systems the scatter effect may be different as it is dependent upon the geometry of irradiation and detection. To investigate these problems the results of the computer simulations have been used to calculate values for the bone mass using detected signals containing only primary photons and also signals made up of the total transmission (primary + scatter photons) for both investigation sites for phantoms 1 to 5 (table 1). These values of bone mass are presented in figure 6.

4. Discussion and conclusions

Since absolute values of bone mass are rarely used and since base levels in most systems are normalized by the use of a calibration phantom, it is the variation between measurements when the patient size changes that is generally important. Several

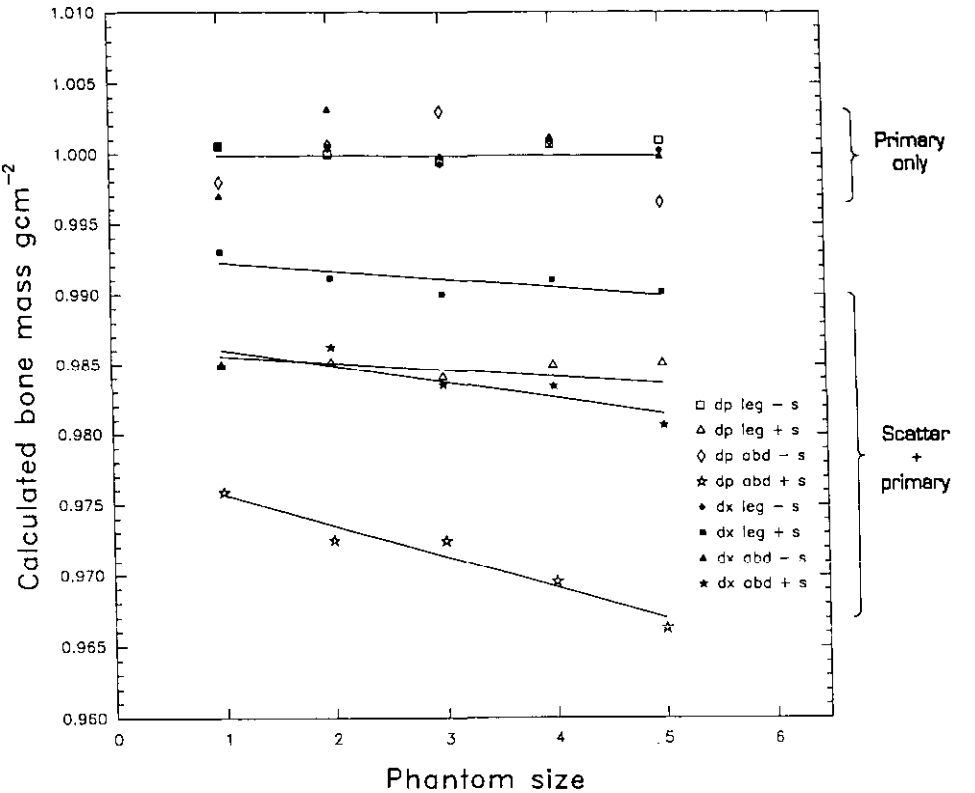

Figure 6. Values of bone mass for different systems, phantom sizes and measurement sites. Values have been calculated with and without the scatter contribution. The straight lines have been fitted using a least squares algorithm.

aspects of the results obtained from DPA and DEXA systems should be considered, for example, serial measurements on any type of system and the effects of patient changes, comparative measurements between different systems, or differing conditions of calibration.

4.1. DPA and DEXA comparison

The major difference between the DPA and DEXA systems are their radiation sources. In order to maintain count rate the collimation on the isotope system is generally less rigorous and thus the detected signal contains a greater proportion of scattered counts. Figure 6 shows the variation in the bone density estimates for identical phantom conditions using the two different systems. It can be seen that for an identical phantom both DPA and DEXA give, within statistical limits, the same result when primary radiation only is considered. When scatter is included the measured bone density is reduced and the magnitude of this reduction depends upon the system and the patient size. A 0.5–3.5% reduction can be expected between system types. If comparisons between measurements on different systems are being made, part of this deficit would still be present even if the scatter in an individual system had been 'removed' by calibration. From figure 6 the remaining deficit would be 0.8% for the

femoral neck and between 0.9 and 1.5% for the abdomen. This effect will be seen when comparing DEXA measured bone density with a previous data base evaluated with DPA, for example.

4.2. Effect of phantom size

Serial measurements, separated by three to four months, are taken in patient studies. During this period the patient might lose or gain weight and alterations in patient dimensions are possible. Figure 6 shows the variation in bone mass estimates when changes occur in phantom size with no change in bone density. Even if the 'scatter effect' had been removed by calibration with a phantom of known density, there would still remain the effect that would be introduced by a calibration phantom of a different size to the patient under investigation. From figure 6 it can be seen that this effect might range from 0.5% (DEXA femoral neck) to 1% (DPA lumbar spine).

Dual energy absorptiometry is the most frequently used method for estimating bone density. If absolute bone mass values or changes in measured values are to be used then the measurement conditions become important in defining the degree of bias introduced due to the effect of scatter. It has been shown that the systems studied are not very sensitive to the degree of scatter and are likely to introduce errors of the order of 1%. However, since density changes reflect bone strength changes of a factor of two greater (Mosekilde *et al* 1987, Britton and Davie 1990), it is thought that a change of 3% could be significant. Thus, when making serial measurements patient size should be taken into account or when comparing measured values with previously obtained data sets the conditions of measurement should be considered.

Résumé

Mesure pour absorption photonique de la densité osseuse en présence de rayonnement diffusé.

Des mesures de densité osseuse sont fréquemment réalisées en utilisant les techniques d'absorptiométrie photonique. L'analyse des données collectées par ces techniques dépend des signaux fournis par le détecteur en l'absence de rayonnement diffusé. En pratique la collimation du détecteur et de la source conduit à la détection de niveaux élevés de rayonnement diffusé. Une analyse du problème en utilisant des modélisations par ordinateur du transport des photons, a montré que les systèmes classiques sont raisonnablement insensibles à la contribution du diffusé sauf quand des changements du patient surviennent au cours d'une longue série de mesure ou quand de nouveaux résultats par DEXA sont comparés avec ceux obtenus sur des systèmes plus anciens tels que DPA. Ceci est fréquemment le cas puisque la majeure partie des données du corps sont reliées à des séries de mesure de densité osseuse obtenues avec DPA. L'inclusion de rayonnement diffusé dans les calculs de densité osseuse peut conduire à une réduction de 0.5% à 3.5% entre les types de systèmes. Des changements dans la taille des patients pourraient conduire à une réduction de la densité osseuse de 0.5% (mesure du col fémur) à 1% (mesure de la colonne lombaire).

Zusammenfassung

Photonabsorptionsmessungen der Knochendichte bei Vorhandensein von Streustrahlung.

Messungen der Knochendichte werden häufig durchgeführt unter Verwendung photoabsorptiometrischer Verfahren. Die Analyse der gesammelten Daten hängt in diesem Falle ab von streufreien Detektorsignalen. In der Praxis führt die Kollimierung von Detektor und Quelle zu hohen Streustrahlenanteilen. Eine Analyse dieses Problems mit Hilfe von Rechenmodellen des Photonentransports zeigt, daß die üblicherweise verwendeten Systeme ziemlich unempfindlich gegenüber den Streuanteilen sind, außer wenn

Änderungen der Patientendaten auftreten während einer langen Meßserie oder wenn neue Ergebnisse, die man unter Verwendung von DEXA-Systemen erhält, verglichen werden mit den Ergebnisse, die man mit älteren Systemen, wie z.B. DPA erhält. Dies ist häufig der Fall, da der Hauptanteil der Daten bezüglich Serienmessungen der Knochendichte mit DPA-Systemen erhalten wurde. Die Einbeziehung der Streustrahlung in die Berechnungen der Knochendichte kann zu einer 0.5–3.5% Reduzierung zwischen den Systemtypen führen. Änderungen der Patientendaten kann zu einer Reduzierung der Knochendichte von 0.5% (bei Messungen im Bereich des Oberschenkelhalsknochens) bis 1% (bei Messungen im Bereich der Lendenwirbelsäule) führen.

References

Birch R, Marshall M and Ardran G M 1979 Catalogue of spectral data for diagnostic x-rays *HPA Scientific Report Series 30* (York: HPA)

Britton J M and Davie M W J 1990 Mechanical properties of bone from iliac crest and relationship to L5 vertebral bone *Bone* **11** 21–8

Cameron J R and Sorenson J 1963 Measurement of bone mineral *in vivo*: an improved method *Science* **142** 230–2

Cashwell E D and Everett C J 1959 *A Practical Manual on the Monte Carlo Method For Random Walk Problems* (New York: Pergamon)

Cullum I D, Ell P J and Ryder J P 1989 X-ray absorptiometry—a new method for the measurement of bone density *Br. J. Radiol.* **62** 587–92

Haddaway M, Grantham S and Davie M W J 1989 Contribution of cortical and trabecular bone to density in lumbar vertebrae and relationship of trabecular density to mechanical strength *Osteoporosis and Bone Mineral Measurement* ed E F J Ring, W D Evans and A S Dixon (York: IPSM) pp 186, 191

Hubbell J H 1969 Photon cross sections, attenuation coefficients and energy absorption coefficients for 10 keV to 100 GeV *NSRDS-NBS* **29**

ICRP 1975 Report of the task group on reference man *ICRP Publication* 23

Koligliatis T 1990 A scattering method for bone density measurements with polychromatic sources *PhD Thesis* University of London, London, UK

Mosekilde L, Mosekilde L and Danielson C C 1987 Biomechanical competence of vertebral trabecular bone in relation to ash density and age in normal individuals *Bone* **8** 79–85

Raeside D E 1976 Monte Carlo principles and applications *Phys. Med. Biol.* **21** 181–97

Roos B O and Sköldborn H 1974 Dual photon absorptiometry in lumbar vertebrae. I. theory and method *Acta Radiol. Ther. Phys. Biol.* **13** 266–80

Speller R D and Horrocks J 1988 A monte carlo study of multiple scatter effects in Compton scatter density measurements *Med. Phys.* **15** 707–12

Speller R D, Royle G J and Horrocks J A 1989 Review article: instrumentation and techniques in bone density measurements *J. Phys. E: Sci. Instrum.* **22** 202–14

Storm E and Israel H I 1970 Photon cross-sections from 1 keV to 100 MeV for elements $Z = 1$ to $Z = 100$ *Nuclear Data Tables* A **7** 565–681

Williamson J F and Morin R L 1983 An efficient method of randomly sampling the coherent angular scattering distribution *Phys. Med. Biol.* **28** 57–62